KAWASAKI STEEL TECHNICAL REPORT
No.19 (November 1988)
Steel Pipe

Automatic Inverse Pole Figure Measurement in Steel by Energy-Dispersive X-Ray Diffraction

Michio Katayama, Masato Shimizu, Chizuko Maeda

Synopsis :
Energy dispersive X-ray diffraction (EDXRD) has been performed by measurement of diffracted white X-rays with the aid of a solid state detector (SSD) connected to a multichannel pulse-height analyzer (MCA). In this method, the fluorescent X-ray spectrum and several Bragg reflections can be recorded simultaneously. The newly developed measurement system has been applied to (1) a swift and automatic texture analysis in steel specimens and (2) depth profile measurement of reflection intensities of cold and hot rolled steels and study on coated steel surface.

The body can be viewed from the next page.

Automatic Inverse Pole Figure Measurement in Steel by Energy-Dispersive X-Ray Diffraction*

Michio Katayama
Senior Researcher, Instrumentation & Analytical Science Research Center, Technical Research Div.

Masato Shimizu
Dr. Engi., Senior Researcher, Instrumentation & Analytical Science Research Center, Technical Research Div.

Chizuko Maeda
Researcher, Instrumentation & Analytical Science Research Center, Technical Research Div.

Synopsis:

Energy dispersive X-ray diffraction (EDXRD) has been performed by measurement of diffracted white X-rays with the aid of a solid state detector (SSD) connected to a multichannel pulse-height analyzer (MCA). In this method, the fluorescent X-ray spectrum and several Bragg reflections can be recorded simultaneously.

The newly developed measurement system has been applied to (1) a swift and automatic texture analysis in steel specimens and (2) depth profile measurement of reflection intensities of cold and hot rolled steels and study on coated steel surface.

1 Introduction

As a result of improvements in the resolution of the solid state detector (SSD) in recent years, the energy-dispersive X-ray diffraction (EDXRD), which is combined with the multichannel pulse-height analyzer (MCA), has been widely used. The EDXRD system without performing an angle scan of the sample and detector as in the conventional angle-dispersive X-ray diffraction (ADXRD), can obtain plural diffraction patterns simultaneously by simply fixing the goniometer at an arbitrary reflection geometry ($\theta/2\theta$—angles between incident beams and samples/diffraction angles).[1] Since fluorescent X-rays are also excited from samples, an element analysis is also possible.

This paper introduces the automatic inverse pole figure measuring system[2], recently developed with the aim of easily and quickly obtaining the textures of steel materials,[3] and further describes various other functions of this system such as the depth profile and the evaluation as $\bar{r}$-value of the texture of cold rolled steel sheets and also the texture measurement at a certain depth and the thickness measurement of the plated layer of a coated steel sheet using fluorescent X-rays, which are simultaneously excited.[4]

2 Measurement Principles and Configuration

2.1 Energy-Dispersive X-Ray Diffraction

From Bragg's condition X-ray energy (E) can be expressed as

$$E = \frac{hc}{2d \sin\theta} = \frac{6.199}{d \sin\theta} \quad \cdots\cdots (1)$$

where θ is an incident angle to the surface of the sample.

In the present method, intensities of diffracted planes (hkl) within the range of the energy detector can be simultaneously obtained without angle-scanning of the goniometer as in the case of the conventional angle-

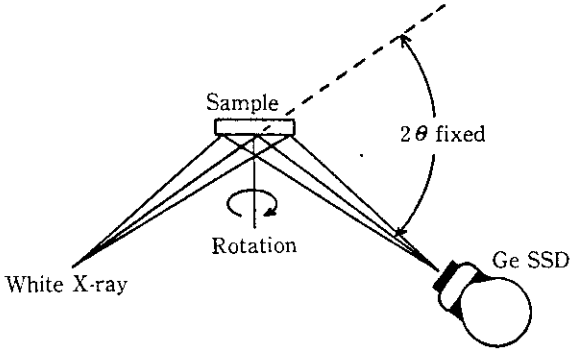

Fig. 1 Principle of the energy-dispersive X-ray diffraction method

* Originally published in *Kawasaki Steel Giho*, 20(1988)1, pp. 42-47

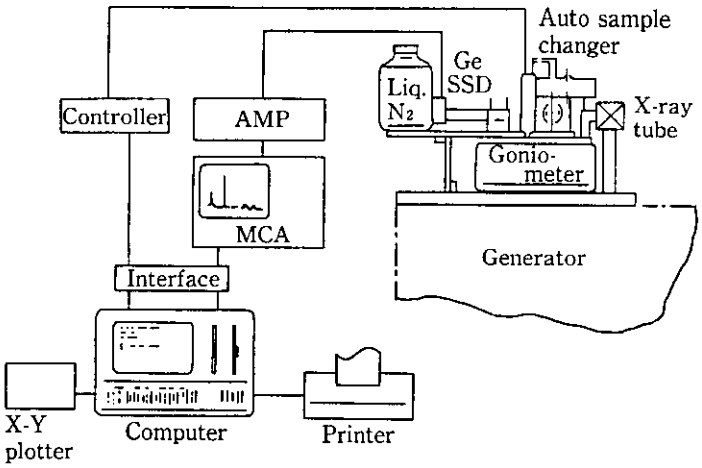

Fig. 2 Schematic representation of the energy-dispersive X-ray diffraction system

dispersive X-ray diffraction. The schematic diagram of this is shown in **Fig. 1**.

2.2 Configuration of Measuring System

The block diagram of the recently developed automatic inverse pole figure measurement system by energy-dispersive X-ray diffraction is shown in **Fig. 2**. This system consists of a 2kW X-ray tube (Cr target), auto-sample-changer, rotary sample stand, Ge-solid state detector (Ge-SSD), goniometer, multichannel pulse-height analyzer (MCA, 4096 ch.), personal computer and accessory printer and X-Y plotter.

3 Examination of Present System

3.1 Diffraction Pattern of α-Fe

Diffraction pattern of a randomly oriented sample (α-Fe) measured by Cr white X-rays for 5 min at $2\theta = 30°$ is shown in **Fig. 3**. Peaks at the left end are Cr Kα from the X-ray tube, and Fe Kα and Kβ from the sample. The peak intensity/background ratio of (211) which is the most intense among the 10 diffraction patterns of α-Fe low-index planes is 34, and that of (222) is 4. Relative intensities of (200), (211) and (222) planes to the strongest peak of (110) plane are 58, 181 and 21 respectively. On the other hand, those by the conventional diffraction method using characteristic X-ray (Mo Kα) are 16, 33, and about 3 for (200), (211) and (222), thereby indicating that relative intensity ratio have significantly improved. The reason for this is the effect of the intensity distribution from 20 keV to 40 keV of the white X-rays used.

3.2 Comparison between EDXRD

ND axis densities of 3-time repetitive measurements

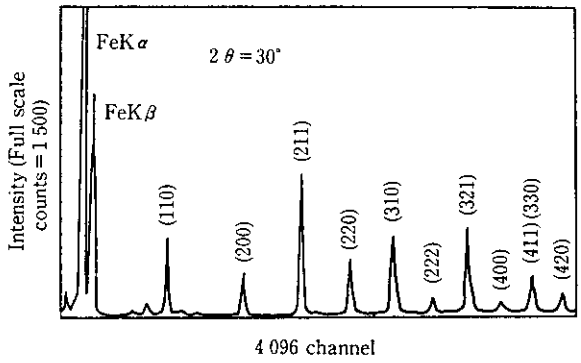

Fig. 3 Diffraction spectrum of a randomly oriented steel sheet

of the main diffraction planes of five kinds of cold rolled steel sheets by the conventional ADXRD system and the present EDXRD system are shown in **Fig. 4**. The dispersion came in the range of 6 to 9% with the correlation coefficients of 0.975 to 0.992, thereby indicating a good agreement with values obtained by the conventional system.

3.3 Preparation of Inverse Pole Figure

Since the quality of several steel products such as deep drawable steel sheets and electrical steel sheets can be improved by controlling their texture, there have been many studies made on texture formation. For deep-drawing-quality steel sheet ND//$\langle hkl \rangle$ (pole density of the lattice plane) of main diffraction peaks are usually obtained. Therefore, the inverse pole figures are not necessarily demanded for all the samples measured by the present system. In the present system, it is so arranged that inverse pole figures are arbitrarily executed by batch processing as shown in **Fig. 5**.

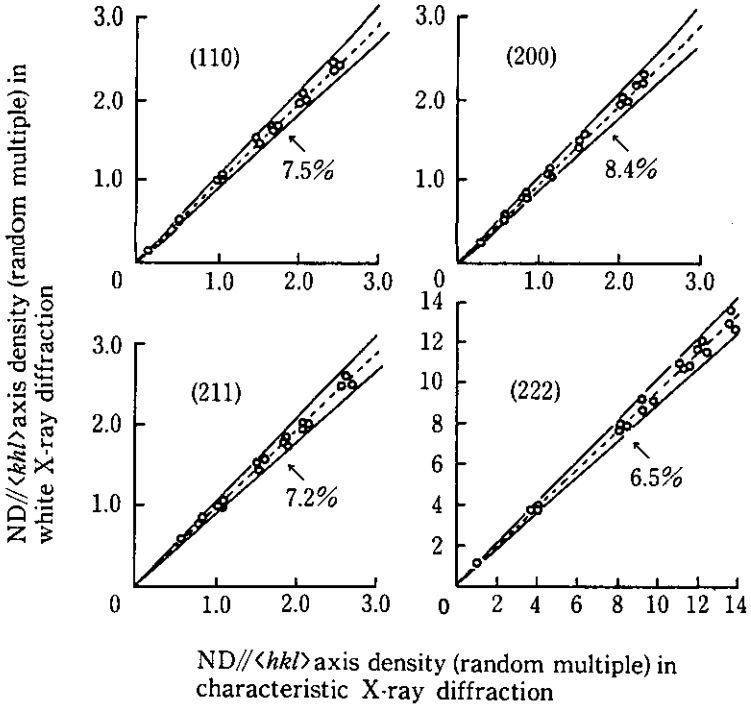

Fig. 4 Correlation between diffraction intensities obtained by the EDXRD method and by the ADXRD method

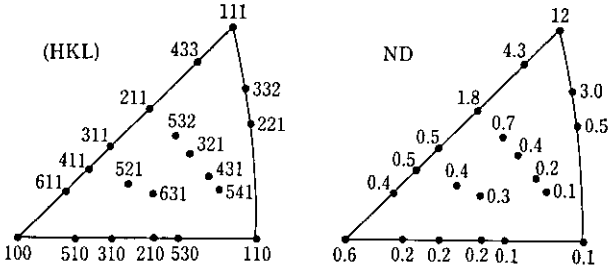

Fig. 5 A plotter-output of ND//⟨*hkl*⟩ axis density

3.4 Penetration Depth of X-Rays

The effective penetration depth of X-rays can be calculated by Eq. (2).[5]

$$t = \frac{\sin\theta}{2\mu}\ln\left(\frac{1}{1-\mathrm{Gx}}\right) \quad \cdots\cdots(2)$$

where Gx: Intensity ratio of thin film to sufficiently thick sample

μ: Linear absorption coefficient of the material for X-rays

t: Penetration depth of X-rays

The difference in the X-ray penetration depth (Gx = 0.99) of α-Fe between the conventional ADXRD method using Mo Kα and the present EDXRD is shown in **Table 1**. In the ADXRD method, X-ray penetration depth is 13 and 40 μm for crystal planes (110) and (411) respectively. Whereas in the EDXRD method, it is 7 μm and 152 μm for crystal planes (110) and (411) respectively, since the values of $E(\lambda)$ are different which contributes to the respective diffration planes, thus indicating very great crystal plane dependence. Therefore, with EDXRD method, it is possible to freely control the X-ray penetration depth within the energy range of white X-ray by changing the diffraction geometry ($\theta/2\theta$).

Table 1 Effective penetration depths in iron by two methods

Gx=0.99	ADXRD		EDXRD $2\theta=30°$	
(*hkl*)	2θ(deg.)	t(μm)	λ(Å)	t(μm)
110	20.2	13	1.052	7
200	28.6	20	0.743	19
211	35.4	24	0.607	33
220	41.0	27	0.526	49
310	46.2	30	0.469	67
222	50.8	32	0.429	83
321	55.3	36	0.397	109
400	59.4	38	0.360	138
411, 330	63.4	40	0.348	152

4 Measurement of Texture of Deep Drawing Quality Steel Sheets

4.1 Texture Dependence of $\bar{r}$-Value

Cold rolled steel sheets are now being used in large quantities as base sheets of various coated steel sheets for automobiles and home electric appliances. Their deep drawability improves as their Lankford value (r-value) becomes larger.[6] Their formability is closely related to crystallographic orientation, and it is considered that $\{111\}\langle uvw\rangle$ orientation is a great advantage for deep drawability, conversely the orientations with (100) and (110) plane are not. Matsudo, et al. have proposed that $\bar{r}$-value has a linear correlation to intensity ratio with (222) and (200).[7] **Figure 6** shows the relation with intensity ratio, (222)/(200), and $\bar{r}$-value measured by the present system. The $\bar{r}$-value can be simply estimated from the value (222)/(200) with the aid of Fig. 6. For instance, if measured values (222)/(200) are 70.0, the estimated $\bar{r}$-value will come to be 2.4, and thus there is no need for conducting the tensile test. In this way, the present system can be effectively used as an evaluation technique for index preparation during the development stage, and also for quality control of test materials and production line materials.

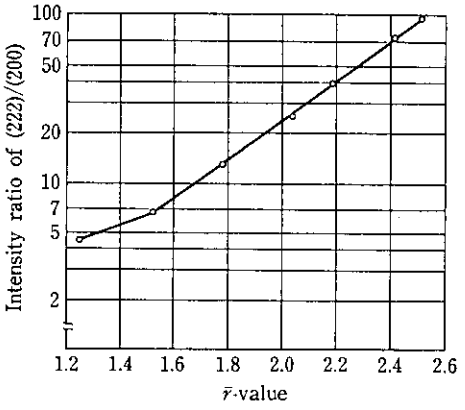

Fig. 6 Texture dependence of $\bar{r}$-value of the cold rolled steel sheet

4.2 Measurement of Depth Profile of Texture

Texture of hot rolled steel sheet has an important effect upon that of successively cold rolled steel sheet. In general, the hot rolled steel develops conspicuous texture changes from the surface to the center of the sheet. At the surface layer, (110) orientation is strong and other (200), (211) and (222) orientations are weak. At the central layer, the reverse trend is predominant, and $\langle 110\rangle$ fiber texture is developed. On the measurement of the depth profile of the texture in a hot rolled sheet, the conventional ADXRD method demands sequential grinding from the surface, because of impossibility of controlling the penetration depth of incident X-rays, whereas in the present system, the penetration depth of X-rays can be arbitrarily changed by changing the diffraction geometry ($\theta/2\theta$). As an example, the depth profile of the texture of a cold rolled steel sheet is shown in **Fig. 7**. As can be clearly seen from the figure, the relative intensities from various diffraction planes are almost constant, even if the penetration depth is changed.

Figure 8 shows the depth profile of the texture near the surface of a rolled steel sheet by changing the X-ray penetration depth in the present system. At a depth of about 10 μm from the steel surface, an accumulation of (110) orientation is observed, but (200) orientation conversely tends to gradually increase towards the central

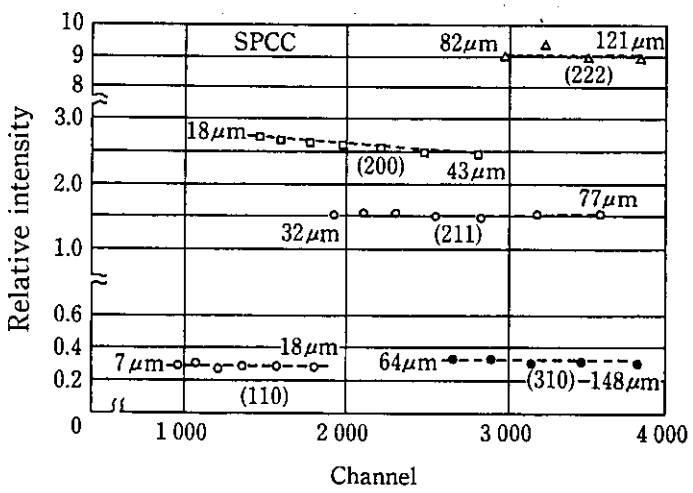

Fig. 7 $\{hkl\}$//ND reflection intensities of a cold rolled sheet at various diffraction angles (Penetration depths are shown.)

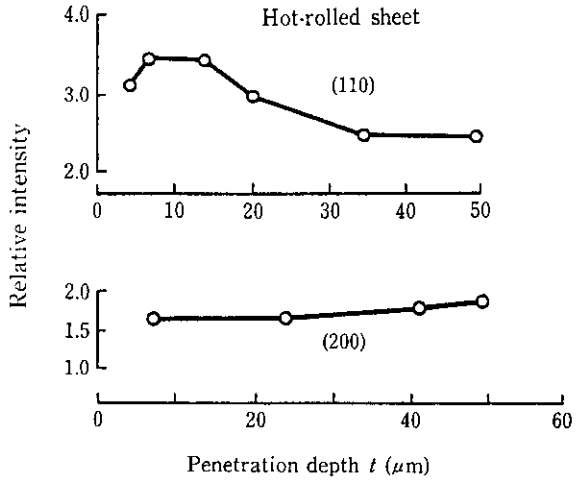

Fig. 8 Depth profiles of $\{hkl\}$//ND reflection intensities in a hot-rolled steel sheet

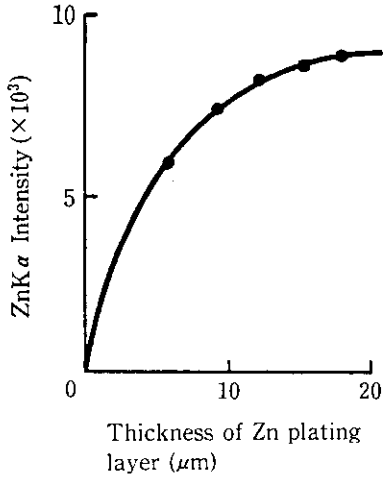

Fig. 10 Intensities of fluorescent X-ray of ZnKα in several kinds of plating thickness of the hot-dip galvanized steel sheet

layer. Such accumulation of (110) is influenced by the hot rolling conditions and component of the material.

5 Texture of Hot-Dip Galvanized Steel Sheet

5.1 Thickness Measurement of Zn Plating Layer

It was described previously that in the present system, not only diffracted X-rays but also fluorescent X-rays can simultaneously be detected. X-ray diffraction patterns of a hot-dip galvanized steel sheet and fluorescent X-ray spectra of Zn Kα and Kβ are shown in **Fig. 9**. For the measurement of the thickness of the Zn plating layer Zn Kα (8.63 keV) was used and the calibration curve shown in **Fig. 10** was made, where horizontal coordinates show the thickness of the Zn plating layers determined by the cross sectional micrograph of several kinds of Zn plating thicknesses. This result of the thickness measurements can be effectively used also for texture measurement at a fixed penetration depth of a Zn plating layer as follows.

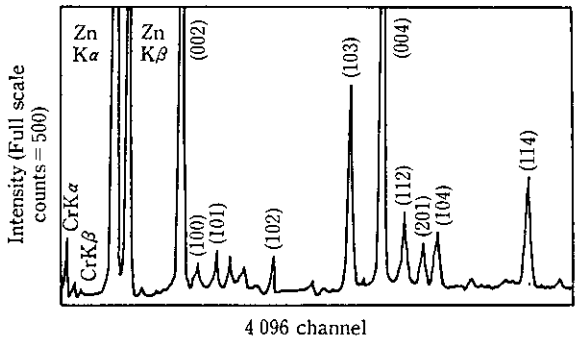

Fig. 9 Fluorescent X-ray spectrum and diffraction pattern of Zn by EDXRD

5.2 Texture Measurement at Fixed Penetration Depth of Zn Plating Layer

Hot-dip Zn plating changes its spangles depending upon the production conditions, and consequently changes its corrosion resistance and glossiness. In general the texture of the Zn plating layer has an effect upon the spangles. The error depending on the crystal plane can be removed by the following EDXRD method with fixed penetration depth. This method adopts the condition of diffraction geometry shown in **Table 2**, which is calculated from Eqs. (1) and (2), after the plating thickness is calculated from Fig. 10. As can be clearly seen from the table, it is necessary to set $\theta/2\theta$ at a higher angle, because lower energy is used as the plating layer becomes thinner, and to set $\theta/2\theta$ at a lower angle as the plating layer becomes thicker. As an example, **Fig. 11** shows the result of measurements made without compensation for penetration depth and with fixed penetration depths which are set up for three kinds of Zn plating thickness differences. The vertical coordinates show the relative intensity of the diffracted X-rays to the Zn powder specimen. The $\theta/2\theta$ fixed measurement at a plating thickness of 6.8 μm showed about a 33% to 15% smaller relative intensity at (102) to (002) than the thickness-compensated measurement. This suggests that although higher energy is contributing to diffraction at the higher index crystal plane on the $\theta/2\theta$ fixed measurement, no significant intensity is obtained, because the plating layer is thinner than the penetration depth. At the plating thickness of 10.2 μm, no conspicuous difference is observed. At 17.5 μm, a difference is observed between (002) and (102), but there is no difference between (100) and (101). In the case of $\theta/2\theta$ fixed measurement, it is supposed that because the plating is so thick, the X-rays have not

Table 2 X-ray energy values and diffraction angles calculated from individual penetration depth of principal lattice planes of Zn

Penetration depth (μm)	Lattice plane (hkl)	Interplaner spacing (d)	Energy (E)	Diffraction angle (2θ)
5	(002)	2.47	13.0	22.2
	(100)	2.31	12.2	25.5
	(101)	2.09	11.6	29.6
	(102)	1.68	10.0	43.2
10	(002)	2.47	19.0	15.2
	(100)	2.31	18.5	16.7
	(101)	2.09	17.0	20.1
	(102)	1.68	15.4	27.7
15	(002)	2.47	23.8	12.1
	(100)	2.31	22.8	13.6
	(101)	2.09	21.7	15.7
	(102)	1.68	19.4	21.9
20	(002)	2.47	28.2	10.2
	(100)	2.31	26.8	11.5
	(101)	2.09	25.8	13.2
	(102)	1.68	23.0	18.4

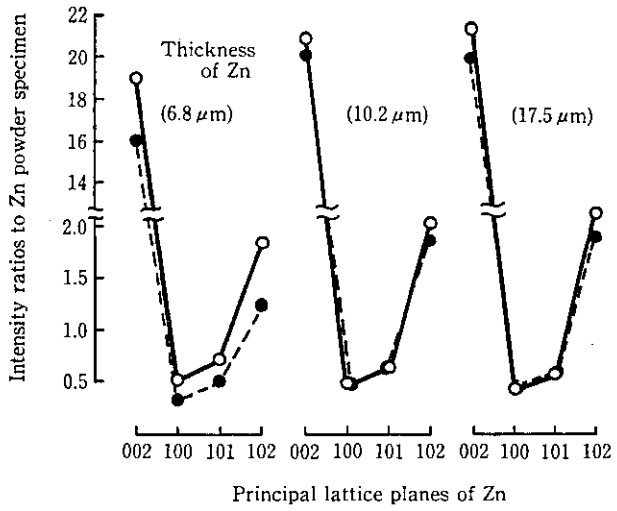

Fig. 11 Relative intensity to Zn powder specimen measured by EDXRD in hot-dip galvanized steel sheets (○ fixed penetration depth measurements, ● fixed scattering angle measurements)

sufficiently penetrated. There is also a possibility that (002) orientation is located near the surface of the sheet, and this matter requires further examination in the future.

6 Conclusions

Through the adoption of the energy-dispersive X-ray diffraction (EDXRD) method which takes the place of the conventional angle-dispersive X-ray diffraction (ADXRD) method, an automatic inverse pole figure measurement system has been developed which permits quick, bulk processing, and the following results have been obtained:

(1) For deep drawing quality steel sheet, the relation between the production conditions and texture has been clarified.

(2) The measurement of the depth profile of the texture has been established without the need to grind the sample.

(3) Further, through the use of fluorescent X-rays which are excited by the sample, the measurement of the plating thickness of hot-dip galvanized steel sheet has been made possible, and texture measurements at fixed X-ray penetration depths corresponding to the plating thickness have also been made possible.

Finally, the authors would like to mention that the EDXRD system has been jointly developed with Rigaku Corp., and they are deeply indebted to that company's staff for their assistance and cooperation.

References

1) L. Gerward, S. Lehn and G. Christiansen: *Texture of Crystalline Solids*, 2(1976), 95
2) M. Katayama, M. Shimizu, M. Konishi, H. Kitagawa, and K. Morimoto: *Tetsu-to-Hagané*, 70(1984)5, S564
3) M. Katayama, M. Shimizu, M. Konishi, H. Kitagawa, and K. Morimoto: "The 21st Symposium on X-ray studies on Mechanical Behavior of Materials", The Society of Materials Science, Japan (1984), p. 117
4) M. Shimizu, M. Katayama, and H. Kitagawa: "Experimental Techniques of Texture Analysis", Deutsche Gesellschaft für Metallkunde, (1986), p. 107-114
5) B. C. Cullity: "Elements of X-ray Diffraction", (1956), [Addison-Wesley Pub. Co., U.S.A.]
6) R. S. Buns and R. H. Heyer: *Sheet Met. Ind.*, 35(1958)372, 261
7) K. Matsudo and T. Shimomura: *Tetsu-to-Hagané*, 56(1970)1, 28